Applied Catalysis B: Environmental 163 (2015) 74–82

Contents lists available at ScienceDirect

Applied Catalysis B: Environmental

journal homepage: www.elsevier.com/locate/apcatb

Steam reforming of acetic acid – A major component in the volatiles formed during gasification of humin

T.M.C. Hoang [a], B. Geerdink [a], J.M. Sturm [b], L. Lefferts [a], K. Seshan [a,*]

[a] Catalytic Processes and Materials, Faculty of Science & Technology, MESA+ Institute for Nanotechnology, University of Twente, 7500 AE Enschede, The Netherlands

[b] Industrial Focus Group XUV Optics, MESA+ Institute for Nanotechnology, University of Twente, 7500 AE Enschede, The Netherlands

ARTICLE INFO

Article history:
Received 4 June 2014
Received in revised form 11 July 2014
Accepted 15 July 2014
Available online 31 July 2014

Keywords:
Steam reforming
Acetic acid
Humin
Nickel
Ceria–zirconia

ABSTRACT

Acetic acid and phenols are the major components of the condensable by-products in the low temperature de-volatilisation stage of humin during gasification. Catalytic steam reforming of acetic acid using supported Ni on ceria-zirconia mixed oxide prepared via the hydrothermal route is discussed. The influence of steam reforming temperatures, steam/carbon ratios were studied. The catalyst showed high activity and good stability. Furthermore, activity improvement was achieved with multiple redox cycles as relevant to recycling the catalysts. Characterisation of the fresh and used catalyst by various techniques (e.g., LEIS, Raman spectroscopy, TPO/TPR) revealed the modification of metal-oxygen bond on the support under the steam reforming conditions. It in turn improved the oxygen mobility of the catalyst.

1. Introduction

Lignocellulosic biomass is addressed as a sustainable alternative to fossil feedstock for transportation fuels and chemicals [1–4]. However, the bio based oils (derived via liquefaction) or chemical building blocks (synthesised via dehydration, fermentation etc.) usually have high oxygen contents. Therefore, to be green, sustainable hydrogen is mandatory in most of these biomass processes for upgrading these products. In our previous study [5], we have demonstrated the generation of hydrogen from humin, a major waste produced during the dehydration of carbohydrates for making bio-chemical platforms (viz. 2,5 hydroxy methyl furan and levulinic acid). Complete conversion of humin could be achieved with selectivity towards synthesis gas of 75% (on carbon basis). The rest of humin was mainly converted to organic volatiles during pre-heating to the gasification temperatures. In order to use the complete carbon content of humin for synthesis gas or hydrogen production, as well as cleaning the gaseous product stream, it is essential to steam reformed this volatile fraction which contains largely phenols, aromatics and acetic acid. Therefore, steam reforming of these molecules should be considered and integrated in the total gasification scheme. Supported Ni catalysts with ceria–zirconia based support for steam reforming of phenolic fraction of the volatiles were developed and reported in our recent publication [6]. The catalyst using ceria–zirconia solid solution as support which was prepared from hydrothermal treatment preceded by co-precipitation showed most promise with the highest activity and stable selectivity to hydrogen (over 30 h time on stream). This catalyst also showed lowest amount of coke deposits. Acetic acid, on the other hand, is notorious for coke formation which is considered the main cause for catalyst deactivation in steam reforming of oxygenates. Thus, the catalyst for steam reforming of the whole volatile fraction should be active and stable for reforming of acetic, too.

Nickel based catalysts are the most widely used in petroleum industry for steam reforming of naphtha and methane. Basagiannis and Verykios reported that Ni showed the highest value of turnover frequency (TOF) among Al_2O_3 supported noble metal catalysts (e.g., Rh, Ru, Pt, Pd) [7]. In the same literature, the authors also noted that the carrier support had a strong influence on the apparent activation energies for the steam reforming reactions Acidic supports such as Al_2O_3 favour cracking and condensation reactions, thus causing the deposition of coke and deactivation of catalyst [7,8]. Addition of basic oxides (e.g., MgO, CeO_2, La_2O_3) to alumina support enhanced the coking resistance thus improving the catalytic activity, stability [7,9]. Other support materials such as ZrO_2, La_2O_3, and CeO_2 have also been used. However, despite the lower acidity in comparison with Al_2O_3, severe coke formation

* Corresponding author. Tel.: +31 53 489 3254; fax: +31 53 489 4683.
E-mail address: k.seshan@utwente.nl (K. Seshan).

http://dx.doi.org/10.1016/j.apcatb.2014.07.046
0926-3373/

Nomenclature

AcOH	Acetic acid
LEIS	Low energy ion scattering
OSC	Oxygen storage capacity
S/C	Steam/Carbon ratio
S-CO/CO_2	Selectivity towards CO or CO_2, respectively
TOF	Turnover frequency
TPO/TPR/TPD	Temperature programmed oxidation/reduction/desorption
(R)WGS	(Reversed) Water gas shift
WHSV	Weight hourly space velocity
X-600/650/700	Conversion of acetic acid at 600 °C, 650 °C and 700 °C, respectively
XPS	X-ray photoemission spectroscopy
XRF	X-ray fluorescence
Y-Acetone/CO/CO_2/H_2	Yield of Acetone, CO, CO_2 or H_2, respectively
TOS	Time on stream

was also observed [10–13] with ZrO_2. Matas Güell et al. reported that the Pt catalyst using CeO_2 support is more stable than that using ZrO_2. This improvement was explained by the facile redox properties of CeO_2 which can help the oxidation of coke deposits with water. In addition, the oxygen storage capacity, one of the important variables for the redox properties of CeO_2, can be further increased by doping other elements such as Zr, Tb, Gd [14,15]. Catalytic activity, redox properties of ceria is enhanced when it is incorporated with Zr. Research about ceria–zirconia supports for hydrogen production from alkanes and oxygenates were recently reviewed by Nahar and Dupont which shows the strong influence of preparation methods on texture, OSC and redox properties of the catalyst thus catalytic activity for steam reforming [15]. Furthermore, reductive/oxidative pre-treatment can also modify the redox properties of ceria–zirconia [16–18] and steam reforming conditions also include reductive/oxidative conditions. In this paper, we studied the performance of Ni supported on ceria-zirconia prepared via hydrothermal route since it showed best activity and stability in steam reforming of m-cresol. In addition, influence of reductive/oxidative treatments (either during the steam reforming or recycling of the catalysts) on its catalytic properties was also investigated.

2. Experimental

2.1. Catalyst preparation

All the chemicals used in this research are analytical grades purchased from Sigma–Aldrich. Ceria–zirconia oxide support was prepared *via* co-precipitation of $Ce(NO_3)_3{\cdot}6H_2O$ and $ZrO(NO_3)_2{\cdot}xH_2O$ with ammonia followed by hydrothermal treatment in 40 wt.% KOH for 24 h. The support was calcined in air at 800 °C for 6 h prior to deposition of Ni via homogeneous deposition precipitation of $Ni(NO_3)_2{\cdot}6H_2O$ with urea. The supported Ni catalyst was then calcined in air at 500 °C, reduced subsequently in 10 vol.% H_2/N_2 at 650 °C for 1 h. Hereby the catalyst is denoted as Ni/HT. In all thermal treatment steps, the total gas flow of 50 cm^3/min and ramping temperature rate of 5 °C/min was used. Details of catalyst synthesis were described elsewhere [6,19].

2.2. Catalytic performance

The catalytic experiments were carried out in an α-alumina fix bed reactor (internal diameter of 4 mm) at atmospheric pressure. The catalyst powder was pressed, crushed and sieved to sizes between 0.3–0.6 mm. The catalytic bed was held in place by two quartz wool plugs. Typically, the catalyst was reduced in situ with 50 cm^3/min flow of 10 vol.% H_2/Argon at 650 °C for 1 h, then purged under the flow of Ar for 30 min before the furnace was set to gasification temperatures (600–700 °C). Aqueous acetic acid solutions were delivered to an evaporator heated to 145 °C by a syringe pump (ISCO Model 500 D). Details are summarised in Table 1. In all cases, the weight hourly space velocities of acetic acid (WHSV) were similar i.e., 25.2 h^{-1}. In the case of using recycled catalyst, each steam reforming run was separated by regeneration step in which the catalyst (from the previous cycle, in the same reactor) was oxidised in 20 vol.% air/Ar (total flow-rate 30 cm^3/min) at 650 °C for 90 min then cooled down to room temperature before used in the next experiment according to the procedure mentioned above. A heating/cooling rate of 10 °C/min was used in all the ramping temperature steps. Ar was also used as internal standard gas for determination of total gas evolving during the steam reforming. Gas outlet stream from the reactor was cooled and separated using a flash condenser cooled by continuous water stream at 15 °C. Gas composition was analysed by an online Varian CP-3800 gas chromatograph. The liquid from the flash condenser was collected every 30 min intervals for the first 2 h TOS and then with the frequency of every 1–2 h. Composition of the condensed phase from the reactor was analysed using a Shimadzu HPLC system with an Animex HPX-87H column and a Refractive Index detector (RID-10D). Mobile phase of H_2SO_4 (0.005 M, 0.6 mL/min) was used for the separation. The column oven was maintained at 35 °C. It took typically 25 minutes for each analysis.

Reaction equations and calculations for conversion, selectivities and yields are given below.

$$CH_3COOH + 2H_2O \rightarrow 2CO_2 + 4H_2 \quad (1)$$

$$CH_3COOH \rightarrow 2H_2 + 2CO \quad (2)$$

$$2CH_3COOH \rightarrow CH_3COCH_3 + H_2O + CO_2 \quad (3)$$

The yield and selectivity gas products were estimated on carbon basis (except for H_2) and from the equations, below:

$$\text{Conversion}(\%) = 100\% \times \frac{n_{AcOHc}}{n_{AcOHf}} = 100\% \times \frac{n_{AcOHf} - n_{AcOHu}}{n_{AcOHf}}$$

$$\text{Yield of } H_2(\%) = 100\% \times \frac{\text{moles of hydrogen produced}}{4 \times \text{moles of acetic acid feed}}$$

$$\text{Yield of } CO/CO_2/CH_4(\%) = 100\% \times \frac{\text{moles of } CO/CO_2/CH_4 \text{ produced}}{2 \times \text{moles of acetic acid feed}}$$

$$\text{Yield of acetone}(\%) = 100\% \times \frac{3 \times \text{moles of acetone produced}}{2 \times \text{moles of acetic acid feed}}$$

$$\text{Selectivit to } CO/CO_2/CH_4(\%) = 100\% \times \frac{\text{moles of } CO/CO_2/CH_4 \text{ produced}}{2 \times \text{moles of acetic acid converted}}$$

Where n_{AcOHf}, n_{AcOHc} and n_{AcOHu} are the moles of acetic acid that was fed to the reactor, converted and unconverted during the reforming, respectively. The amounts of unconverted acetic acid was calculated from HPLC data with the assumption that negligible amount of acetic acid vapour in the gas stream to GC. Thus, condensed liquid volume is theoretically calculated based on the feed concentration and water consumed in Eq. (1). Carbon balance of 97 ± 3% was achieved in all experiments if not specifically mentioned.

Table 1
Process parameters of feed streams to the reactor.

$[AcOH]_{feed}$[a] (g/L)	S/C ratio	F_{liquid}[b] (mL/min)	Catalyst (mg)	Gas flowrate, cm^3/min[c]		
				Ar	AcOH	Steam
104.7	14	0.1	25	25	4.2	120
252.8	5	0.083	50	45	8.4	84

[a] Concentration of acetic acid solution.
[b] Flowrate of acetic acid solution was delivered by the pump to the evaporator.
[c] Gas flow-rate is re-calculated for ambient condition: 20 °C (293 K), 1 atm.

2.3. Characterisation of catalysts

Main characteristics of the fresh catalyst were reported elsewhere (see Hoang et al. [6]) and summarised in Table 2.

For temperature programmed reduction (TPR) or oxidation (TPO), the catalysts (10–50 mg, with grain size of 0.3–0.6 mm) were held between two quartz plugs in a cylinder, α-alumina reactor (4 mm internal diameter), pre-treated in inert gas (Ar or He for TPR or TPO, respectively) at 150 °C for 30 min then cooled down to room temperature prior to the analysis. 5 vol.% H_2/Ar (25 cm^3/min) or 1 vol.% O_2/He (75 cm^3/min) was used as reactive for these analyses, respectively. H_2 consumption was followed by a standard thermal conductivity detector which was calibrated by conducting similar TPR procedure with known amounts of NiO (purity 99.999%, purchased from Sigma Aldrich). In TPO analysis of coke deposits on catalysts, ~6 vol.% of gas stream from the reactor, containing CO or CO_2, was sent to an online methanizer (Model 110 Chassis, SRI Instruments Europe GmbH) where CO and CO_2 were converted to methane. The evolution of methane was monitored and quantified using a FID detector which was calibrated in the same TPO procedure using known amounts of $Al_2(CO_3)_3$ as carbon source. In TPR or TPO measurement, the furnace was heated to 700 °C at the rate of 5 °C/min then kept at that end temperature for 30 min and subsequently cooled down to room temperature (10 °C/min).

Raman measurements were performed in ambient condition using a Bruker Senterra Raman spectrometer (wavenumber 532 cm^{-1}) equipped with a CCD detector. In each scan, samples were exposed to laser power of 5 mW for 1–2 s. The Raman spectra were average of 50–100 scans with spectral resolution 3–5 cm^{-1}.

The Ni dispersion of 3.8% was estimated from CO chemisorption at room temperature (Micromeritics Chemisorb 2750). The fresh catalyst was pre-treated in 10 vol.% H_2/Ar at 650 °C for an hour, then degassed in helium at this temperature for 15 min prior to cooling down in helium to room temperature (rate of 10 °C/min). Transmission electron microscopy was also employed to determine the metal particles size distribution of fresh and used catalysts. However, due to the low contrast between the support and nickel, only few metal nanoparticles were resolved. Therefore, Low-Energy Ion Scattering (LEIS) was used to determine the relative change in surface composition of the catalyst (including Ni). LEIS was performed with commercially available equipment (ION-TOF Qtac^{100} from ION-TOF). A catalyst sample was pressed to a pellet, which was pre-treated with atomic oxygen in order to remove hydrocarbon contamination before introduction in the analysis chamber. Both He and Ne were used as primary ion source, with a dose density of typically 2×10^{14} ion/cm^2 per spectrum.

Table 2
Characteristics of Ni/HT catalyst.

Specific area (m^2/g)	42
Pore volume (cm^3/g)	0.29
Ce/Zr atomic ratio	0.2[a] (0.23[b])
Ni loading (wt.%)	3.2
Metal dispersion (%)	3.8[c]
Surface Ni/Ce/Zr (atomic ratio)[b]	14.7/69.2/16.1
Ce^{3+}/Total Ce (%)	43[b] (80[d])

[a] Based on XRF.
[b] Based on XPS result.
[c] Based on CO chemisorption.
[d] Based on TPR.

3. Results

3.1. Performance of fresh catalyst

The performance of Ni/HT catalyst for steam reforming of acetic acid in the temperature range 600–700 °C is shown in Fig. 1. It can be easily seen that conversion of acetic acid and selectivity to different products strongly depends on the reaction temperature. The catalyst showed very high conversion at the beginning (90–98%, Fig. 1A). However, its activity curve showed rapid initial deactivation, within the first ~4 h TOS. The rate of initial deactivation was strongly dependant on the temperature. For example, at 600 °C, the conversion dropped from ~ 90% to ~50% in 2 h TOS, while at 700 °C the activity loss was only 6%. However, throughout the subsequent 23 h TOS, the conversions dropped ca. 16% for these three reforming temperatures. This slow gradual deactivation seems to be independent of the reforming temperature.

Identified products of steam reforming of acetic acid (Fig. 1B) included CO, CO_2, H_2, acetone and trace amounts of methane. It should be noted that no other hydrocarbons were detected. The highest yield of acetone was obtained at 600 °C in the first 1 h TOS; while at 700 °C, this value was negligible (<0.16%). Since acetone is formed from acetic acid its presence in the product stream indicates that its formation rate is higher than its conversion rate in subsequent reactions to, e.g. syngas, hydrogen. Yields of acetone declined after 4–6 h TOS when the conversion approached steady state. This implies that the initial deactivation of catalyst is strongly connected with the formation of acetone. CO and CO_2 are the main C containing products of steam reforming. When the catalyst reached steady state at 600 °C, selectivity of CO_2 and CO was around 80 and 5% on carbon basis, respectively. Carbon balance in this case was quite poor (88 ± 2%). This implies that besides acetone and CO_x, there are unidentified products (e.g., coke precursors, coke). The highest selectivity towards CO_2 (~ 88% on C basis) at steady state was achieved at reforming temperature of 650 °C. Selectivity to CO_2 at 700 °C was slightly lower than that at 650 °C due to less favourable conditions for the exothermic water gas shift reaction. In both cases (650 & 700 °C), carbon balance of 97 ± 3% was obtained. Yield of hydrogen was proportional to acetic acid conversion and selectivity to CO_x. Due to the highest conversion and yield of H_2, as well as lowest yield of acetone, reforming temperature of 700 °C was selected for further investigations.

As mentioned in the previous section, the temperature had a strong influence on deactivation rate. In this section, impact of steam/carbon ratio on the deactivation rate is investigated. In the case of S/C ratio of 14 (Fig. 1A), the conversion dropped from ~100 to ~76.7% after 30 h TOS. When S/C ratio of 5 was used (Fig. 2), the conversion of acetic acid dropped from ~90 to 63.6%. This amounts to catalyst loss in activity of ~23.3% and 27% with S/C ratio of 14 and 5, respectively. Selectivity toward CO (~15%) was similar in

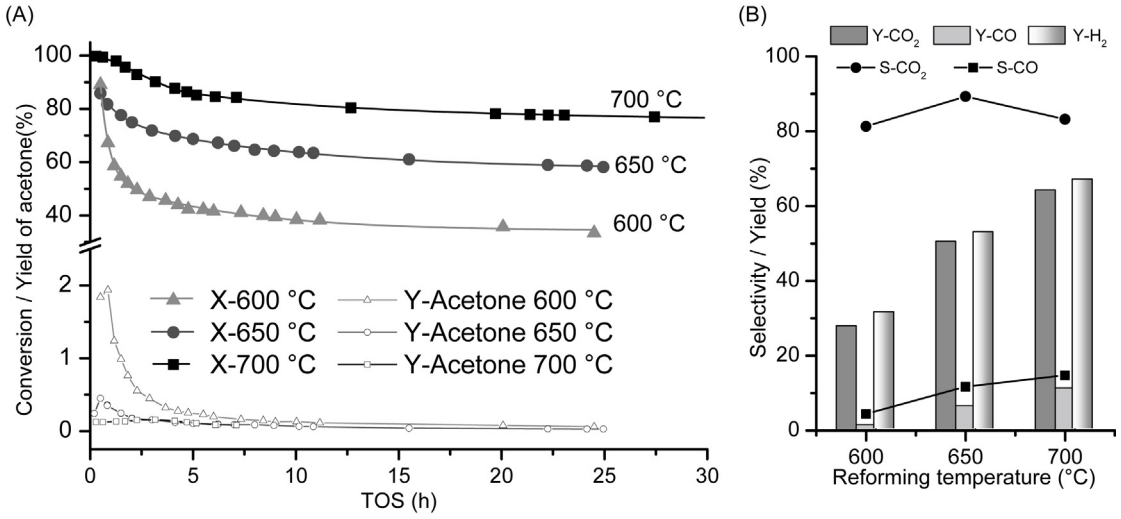

Fig. 1. Influence of reforming temperature on performance of Ni/HT catalyst: A – conversion of AcOH and yield of acetone; B – Selectivity and yield of gaseous products at steady state (conditions: $WHSV_{AcOH}$ = 25.2 h^{-1}; S/C = 14/1, T = 600, 650, 700 °C).

both cases while selectivity to CO_2 was higher for S/C ratio of 14. This is due to the enhanced WGS reaction because of the higher partial pressure of steam. Quantification of coke deposited on the used catalysts showed that the coke contents were similar (1.8 wt.%) in both cases. In agreement with the degree of loss in activity (25% vs. 27%), it seems that the S/C ratio in the range from 5 to 14 has only a very minor impact on the coke content.

The conversion and yields of products from the reforming of AcOH on the bare HT support is shown in Fig. 3. CO_2, CO, CH_4, H_2 and acetone were the detected products here also. Initial conversion of AcOH was as high as ~90% which rapidly decreased to ~4% within 2 h time on stream. Yields of identified products followed the same trend. No further changes in conversion and yields of products were observed after 2 h. Thus the support is strongly deactivated and the low residual yields of products such as CO_2, CH_4, H_2, CO were due to remaining activity of the catalyst/coke or reactions in gas phase. It is also seen that the production of acetone in this case only occurred within the first 2 h TOS, or during the active period of the support.

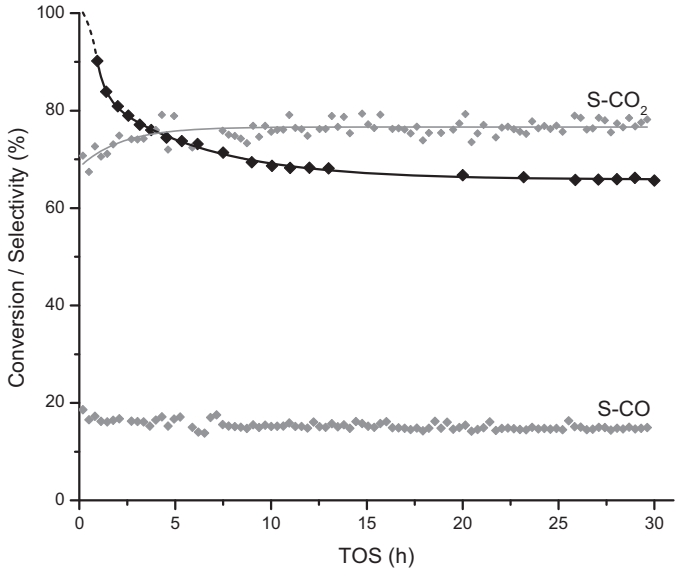

Fig. 2. Steam reforming of AcOH in presence of Ni/HT catalyst with steam to carbon ratio of 5, T = 700 °C, WHSV = 25.2 h^{-1}.

3.2. Influence of catalyst recycles

Fig. 4 shows the influence of catalyst recycles, i.e., deactivation, regeneration by coke combustion, and reduction, on the steam reforming of AcOH with S/C ratio of 14. From Fig. 4A, it can be seen that the conversion with recycled catalyst (Run 5) is higher than the conversion achieved with the fresh catalyst (Run 1). The conversion of AcOH at steady state increased from ~75% to 82%. This increase of conversion is also the direct cause for the increase of H_2 yield (Fig. 4A). For product distribution, at steady state, the selectivity to CO_2 decreased whereas selectivity to CO increased with the recycled catalysts (Fig. 4C). Interestingly, the yields of CO_2 were similar in all these runs but yield of CO is increased clearly (Fig. 4B). This increase in yield of CO corresponds to the gain in conversion. Various characterisations shown further were employed to understand the changes on the catalyst and relate to sequential steam reforming of acetic acid.

3.3. Characterisation of catalysts

Low-energy ion scattering spectroscopy (LEIS) was used to analyse the change in surface composition of the catalyst. This surface sensitive analytical technique allows obtaining information about

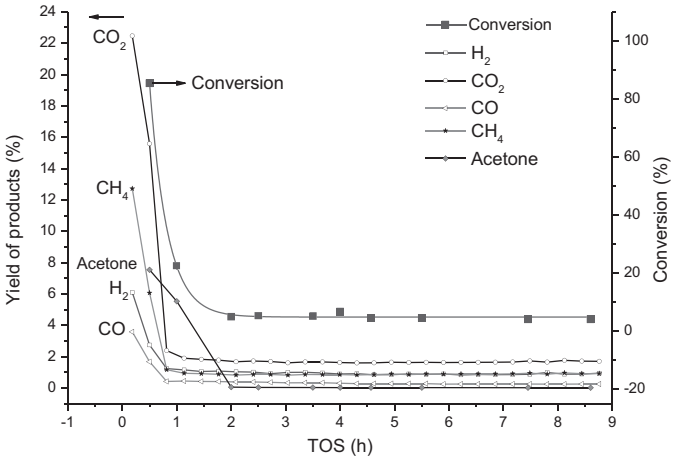

Fig. 3. Reforming of acetic acid on bare HT support $WHSV_{AcOH}$ = 25.2 h^{-1}; S/C = 5; T = 700 °C.

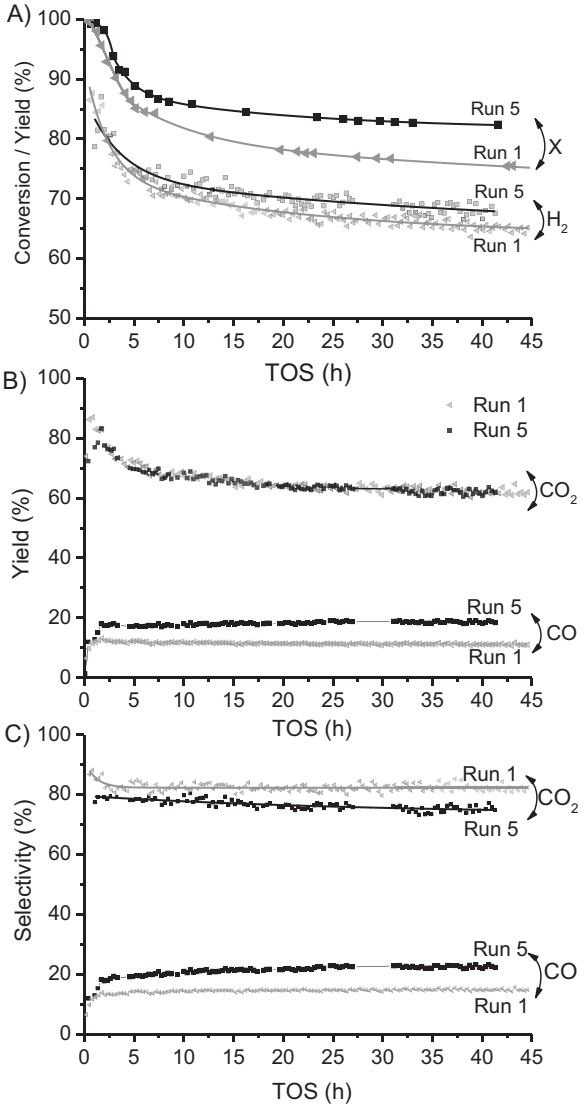

Fig. 4. Influence of catalyst recycle on steam reformoing of AcOH: A – conversions/yields of H_2, B – yields of CO_x, C – selectivity to CO_x. Conditions: T = 700 °C, $WHSV_{AcOH}$ = 25.2 h^{-1}, S/C = 14/1. Label: square and triangle symbols represent Run 5 and Run 1, respectively.

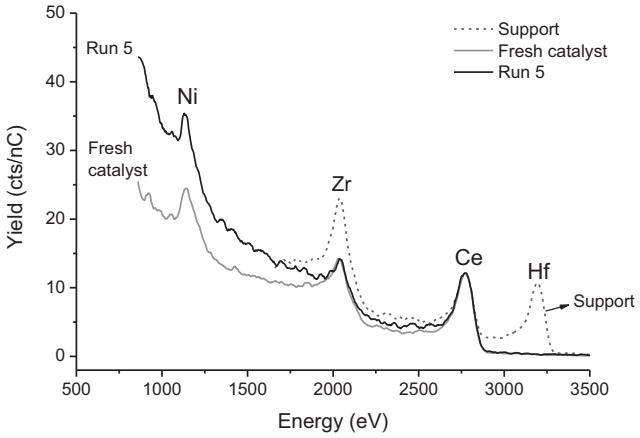

Fig. 5. LEIS spectra of support, fresh and catalyst after Run 5 (reaction conditions for Run 5: S/C = 14/1, T = 700 °C).

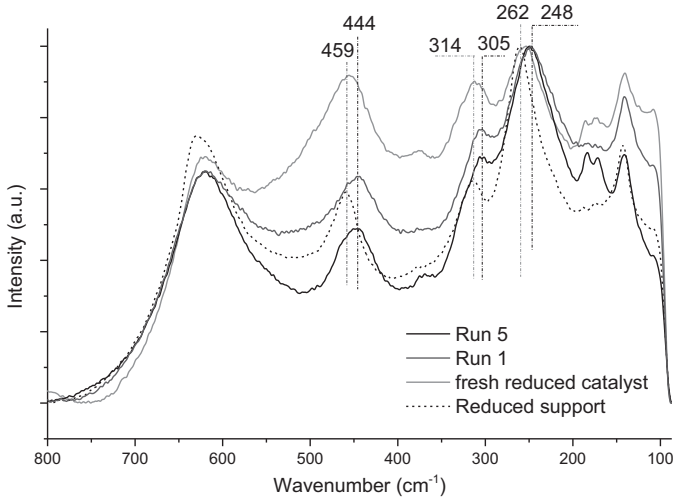

Fig. 6. Raman spectra of fresh and used catalysts after steam reforming (S/C = 14, T = 700 °C). Support was reduced at 650 °C for 1 h. Raman spectra were recorded at ambient conditions (21 °C, 1 bar) with laser wavelength 532 nm and normalised to the peak at ~250 cm^{-1}.

the very first layer of the catalyst surface. Fig. 5 shows the LEIS spectra, obtained by scattering of 5 keV Ne ions, normalised to intensity of the Ce peak. It can easily be observed that the relative Ce/Zr peak ratio of the supported Ni catalysts is higher than that of the bare support. The Ce/Zr ratio of the support is expected to be similar to the bulk Ce/Zr ratio of the catalyst even after Ni deposition. This value (Ce/Zr = 0.2) is derived from XRF result. For the surface composition of the fresh supported Ni catalyst, a Ce/Zr atomic ratio is 0.23 (obtained from XPS). Therefore, the increase of Ce/Zr atomic ratio on the surface observed with LEIS is in agreement with previous results obtained from XPS and XRF. The higher cerium coverage on the surface can be due to two reasons: (i) migration of Ce to the surface during the reduction treatment [20], or (ii) Zr is covered by Ni, in other words Ni precursors deposit preferably on Zr rather than Ce sites during the homogenous deposition precipitation. The disappearance of hafnium (omnipresent impurity in zirconium precursors) on the supported catalyst is also caused by preferential deposition of Ni precursor, albeit its presence on the surface of the corresponding support. Therefore, the latter reason for increase of Ce/Zr ratio is more likely. By comparing the relative ratios of peaks for Ni, Ce and Zr, respectively (Fig. 5), there might be a very slight decrease of Ni and Zr compared with Ce between the fresh catalyst and the catalyst after 5 times of recycle. Therefore, break down of Ni particles, that increases the surface area of Ni nano-particles, thus varying the atomic ratios of Ni to other elements on the surface of the catalyst, is not expected. Additionally, it should be noted that the spectral baseline of the recycled catalyst increased sharply in the low energy range. This effect can be attributed to sputtering of light elements from the catalyst surface. LEIS measurements with He as primary ion showed that the 5 times recycled sample (Run 5) had a 1.2 times larger oxygen surface coverage compared to the fresh catalyst and a small contamination of silicon oxide which comes from the quartz wool used to keep the catalyst bed stationary inside the reactor (7% of the Si surface coverage of a Si wafer exposed to O plasma). The result from time-of-flight measurements of Ne scattering confirms that the increased background of the recycled catalyst was due to sputtering of O and Si (not shown here).

Fig. 6 shows the Raman spectra of the catalysts which are scaled to the band around 250 cm^{-1}. Major spectral features of the Raman spectra from 100 cm^{-1} to 750 cm^{-1} of the catalysts are typical for tetragonal phase for CeO_2-ZrO_2 oxides: ~625 cm^{-1} (A_{1g} mode), ~444–459 cm^{-1} (E_g mode), 314 cm^{-1} (B_{1g} mode), 248–262 cm^{-1}

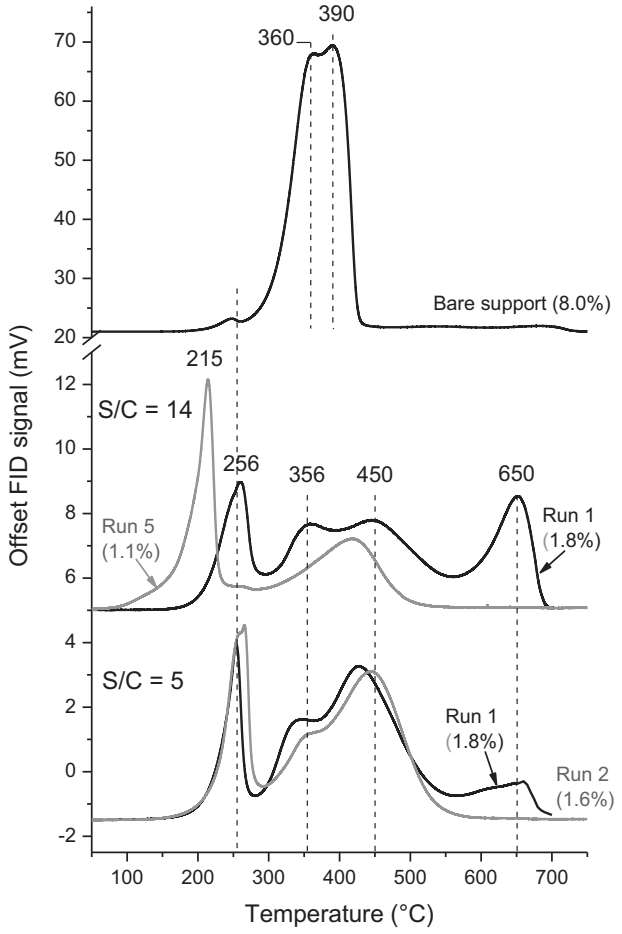

Fig. 7. TPO profile of catalysts normalised to 1 mg weight of catalysts. Numbers in brackets indicate the carbon contents deposited on the catalysts.

(E_g mode) and 140–144 cm^{-1} (B_{1g} mode) [21]. The Raman vibration at 593 cm^{-1} for tetragonal phase which is reported by Hirata [21] is not seen clearly in all spectra. This is probably due to overlap with other bands. Besides, vibrational modes for monoclinic phase were also found, peaks at 376 cm^{-1} (B_g mode), 306 cm^{-1}, 171 cm^{-1}, 183 cm^{-1} (A_g mode). The presence of these bands is also in agreement with the Raman spectrum of the non-reduced support. It can be seen from Fig. 6 that the E_g vibration mode (peaks at ~ 460 cm^{-1} and 260 cm^{-1}) of the catalysts after exposing to steam reforming conditions (Run 1 and Run 5) shifted to lower wavenumber (459 cm^{-1} to 444 cm^{-1} and 262 cm^{-1} to 248 cm^{-1}) compared to reduced fresh catalyst or reduced fresh support.

The E_g mode at 444–460 cm^{-1} is assigned to the asymmetric Zr—O—Zr or Ce—O—Ce stretching while the E_g mode at 260 cm^{-1} corresponds to Zr—O stretching [22] or Ce^{3+} [23]. These red shifts imply cation--oxygen stretching becoming weakened. This indicates certain modification of cation–oxygen bond (i.e., lengthening the bond) [22]. Thus, oxygen can become more labile, causing increase in oxygen mobility. The red shift of E_g mode (from 459 cm^{-1} to 444 cm^{-1}) is much larger than those of recycled ceria–zirconia mixed oxides (the samples were exposed to oxidative/reductive sequence) reported in literature [14,17,21,24–28]. We suggest that the redox processes occurring during the steam reforming of acetic acid have stronger influence on modification of the cation–oxygen bonds (Ce or Zr with O) than conventional redox treatment. This aspect will be elucidated later by TPR analysis.

Coke deposits on used catalysts were determined and quantified based on TPO analysis (Fig. 7). The oxidation profile of the coke deposited on the bare support consisted of two significant peaks at 360 °C and 390 °C and a low-intensity peak at ~250 °C. The coke deposited on the catalysts after the first reforming cycle with both steam/carbon ratios (5 and 14) was very similar in both carbon contents and oxidation profile. These consist 4 oxidation temperatures 256 °C, 356 °C, 450 °C and ~650 °C. The peaks at 210–250 °C can be assigned to strongly adsorbed intermediates of acetic acid on the support. This low oxidation temperature of coke deposits in acetic acid reforming was reported by Vagia and Lemonidou [29] and Lemonidu et al. [30]. However, supported Rh on CeO_2–ZrO_2 or CeO_2–ZrO_2 modified with 3 wt.% La catalysts were used in their cases. The peak above at 650 °C on the supported Ni catalyst after the first cycle can be due to the intermediate species which formed in presence of Ni particles. Surprisingly, the coke on recycled catalysts (run 5 for S/C 14 and run 2 for S/C 5) did not contain any coke component that was oxidised at high temperature – at 650 °C (*i.e.*, all the peaks were below 450 °C). Especially for catalyst after run 5, the oxidation temperatures of the coke shifted to much lower temperatures (30–40 °C lower).

The dependency of redox properties of CeO_2–ZrO_2 materials on the reductive/oxidative treatments which is referred as thermal ageing is well-known in literature [16–18,24,31,32]. Reducibility of ceria based oxides can be enhanced by exposing the samples to sequence of deep reductive treatment followed by mild oxidative treatment [17]. Therefore, similar improvements can be expected with the recycled catalysts used in this study since recycling of catalyst includes oxidation of coke followed by a reduction pre-treatment for the next reforming cycle. Therefore, investigating the reducibility of the catalyst can help to explain their catalytic performance in the steam reforming. It should be remarked that most of the research on the influence of thermal ageing so far focussed on the enriched Ce mixed oxide (i.e. Ce molar content > 50%).

TPR profiles of the supports and catalysts are illustrated in Fig. 8. Since the TPR of recycled catalysts were carried out following the TPO (i.e., samples were oxidised in 1 vol.% O_2/He to typically 700 °C then cooled down in Ar to room temperature, to remove the coke deposits on the used catalyst), the fresh catalysts were also pre-treated under the same conditions (i.e. re-oxidised to 700 °C) prior to each TPR experiment to mimic the thermal treatment history. The TPR profile of fresh support has an asymmetric shape centred at ~500 °C. The support that experienced a cycle of redox (reduction to 700 °C followed by re-oxidation to 700 °C) is labelled as support-redox 1 on Fig. 8. TPR profile of the support-redox 1 consists of two peaks at ~320 °C and 483 °C in which the onset of reduction occurred at a lower temperature compared with the fresh support (150 °C vs. 200 °C). TPR profile of the support which had exposure to the steam reforming conditions for 8 h is quite similar to the support-redox 1 except that the reduction initiates at ca. 100 °C and larger part of Ce is reduced at lower temperature range (the range below 420 °C). This phenomenon indicates the reduction of the treated or used support is facilitated, thus improving reducibility. In the other words, the reductive/oxidative recycle modifies the metal (Zr or Ce)–oxygen bonds, making oxygen more labile. This associates with the oxygen mobility in the lattice of the materials, leading to facile Ce^{4+}/Ce^{3+} redox reaction. Therefore, the thermal ageing treatment (viz. reduction/oxidation of the support in H_2 or O_2, respectively) or the reductive/oxidative condition during steam reforming gives improvement to the oxygen mobility in the support. About 80% ceria is reduced to Ce^{3+} by the end of the TPR experiments for bare supports. This result is in coincidence with literature [17].

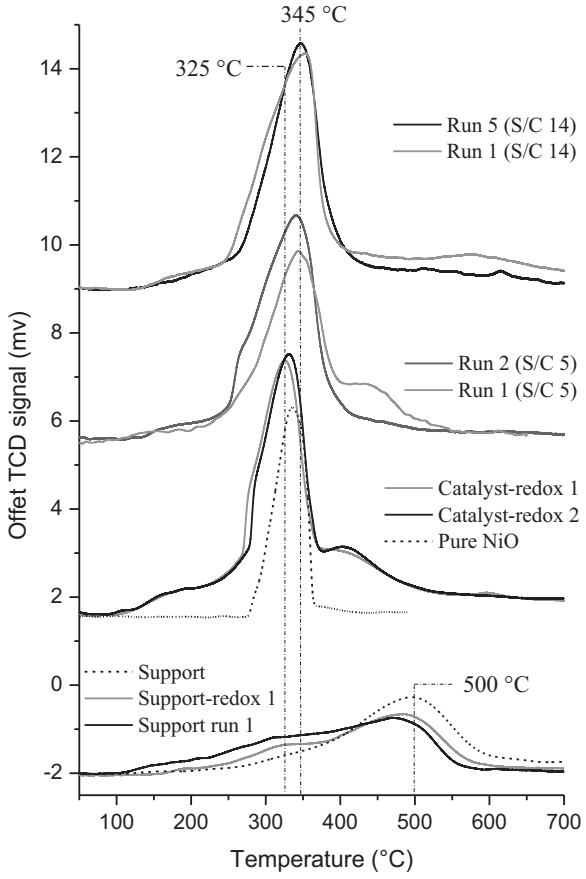

Fig. 8. TPR profiles of catalysts. The intensity of TPR signal was scaled to those for 50 mg of catalysts and TPR signal of NiO was normalised to the same amount of NiO in the catalyst. Support-redox 1, catalyst redox 1 and 2 are fresh support and catalyst which experienced sequence of re-oxidation followed by TPR 1 and 2 times, respectively. Used support, run 1, 2, 5 are those obtained after TPO analysis.

Secondly, for the supported Ni catalysts reduction was initiated at relatively lower temperature (~100 °C) and gradually increased until ~270 °C. Then the reduction sharply increased and showed an asymmetric peak at 325–345 °C. This peak can be related to reduction of bulk NiO on the catalyst since pure NiO (Sigma–Aldrich, large particle size) also showed a strong reduction peak in this temperature range. Additionally, a broad reduction peak at 420–435 °C was found in some cases. Combining with the TPR profile of the support, the broad, asymmetric reduction area beneath the sharp peak at 325–345 °C which peaks at 420–435 °C and spans from ~100 to the end of the temperature program (700 °C) is mainly attributed to the reduction of the Ce–Zr support which is promoted by the presence of Ni. In the case of thermally aged catalysts (catalyst redox 1 and 2) their reduction profiles are quite similar. This indicates that the repeated redox treatment in O_2 and H_2 does not cause further significant changes in reducibility of the catalyst after the first reduction-oxidation cycle. However, the recycled catalysts, which had been exposed to the steam reforming conditions, show some differences compared with the thermally aged catalysts. It can be seen that the highest reduction peak becomes broader and shift to higher temperature from 325 °C to 345 °C. Remarkably, the peaks for support reduction become less distinct and merge with the main peak, making the overlapped total peak shift to 345 °C (the Run 2 and Run 5 catalyst with S/C ratio of 5 and 14, respectively). This demonstrates the more facile reduction of the recycled catalysts. Total H_2 consumption of all supported Ni catalysts (fresh and recycled catalysts) varied only within the machine error. The

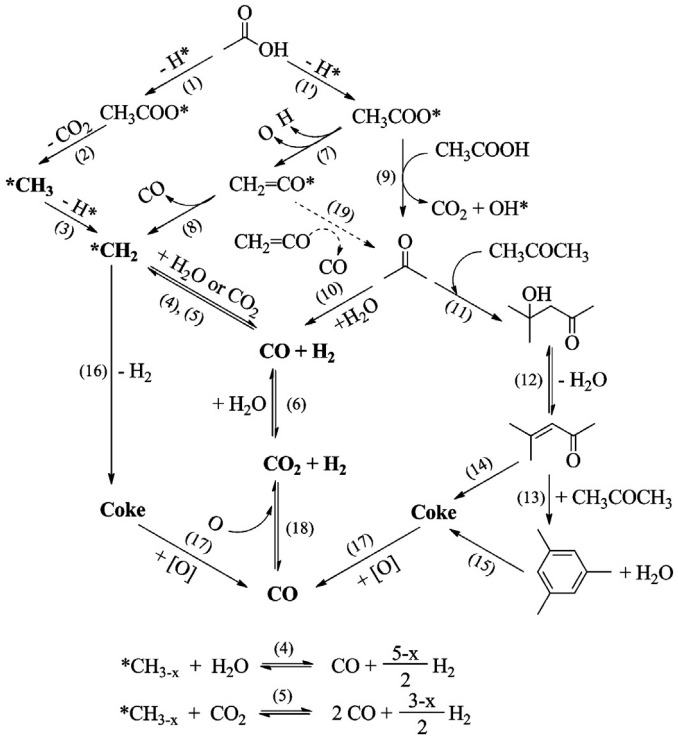

Scheme 1. Reaction pathways occurring in steam reforming of acetic acid.

Ce^{3+}/total Ce ratios were estimated at 80 ± 6% with the assumption that all Ni was completely reduced.

4. Discussion

Reaction pathways which occur in catalytic steam reforming of acetic acid is illustrated in Scheme 1, taking in to account the works reported by Lemonidou et al. [30], Takanabe et al. [10,33], Pestman et al. [34], and Barteau's group [35,36]. In the case of steam reforming in presence of only oxide supports (e.g. ZrO_2, CeO_2, Al_2O_3) conversion of acetic acid through the formation of acetone is favourable. Further condensation of acetone via reaction (11)–(14) is believed to be the main cause for coke formation on the support, blocking the active sites and leading to the deactivation of catalyst. Both acidic and basic sites are known to activate the formation of acetone from acetic acid. However, basic supports such as CeO_2, La_2O_3 or CeO_2/MnO_2 solid solutions are more active than acidic supports for acetone formation [7]. In this study, the bare support itself showed high initial activity for conversion of acetic acid to acetone (compared with the non-catalytic thermal steam reforming) and the catalyst was strongly deactivated (conversion 90% vs. 4%). High yields of CO_2 and CH_4 in the beginning suggests that conversion of acetic acid follows reactions (1), (2) and (9). Yields of CH_4 and H_2 decline faster than that for acetone. This indicates the limited number of active sites on the support for forming $*CH_x$ and these sites are quickly blocked by coke formation probably *via* reaction (16). Active sites for acetone formation, reaction (9), lasted for longer time (~2 h). The poor carbon balance achieved in the case of reforming on bare support implies the large amounts of AcOH or active carbon species (e.g., $*CH_{3-x}$, acetone) were further converted into unidentified products which includes coke deposits. This explains the high coke content in this case (C 8 wt.% – Fig. 8). The accumulation of coke on the support blocks the active sites on the catalysts and inhibits further conversion of AcOH. At the end when all the active sites are blocked, the conversion of acetic acid is just thermal or due to activity of the coke.

In the case of Ce-ZrO_2 supported Ni catalysts, the conversion of AcOH was maintained above 75% after 45 h TOS with stable selectivity to CO_x (almost 100%). Therefore, reforming capability of the catalyst is attributed mainly to Ni metal. The rapid initial deactivation of the catalyst observed in all the experiments is assigned to the deactivation of support activity which is mainly due to accumulation of coke and strongly adsorbed species on the support surface. Ni particles can help with the reforming of acetone formed on support within the proximity of Ni particles to syngas via reaction (10). This explains the very low yield of acetone in the case of supported Ni catalyst compared with reforming in presence of bare support (Figs. 1 and 3). In addition, when steam reforming acetone at 700 °C with WHSV 6.96 h^{-1} with this catalyst (not shown here), total yield of CO_x and CH_4 ~ 95 ± 2% (yield of CH_4 ~ 1%) was achieved. Thus, the catalyst is capable of reforming acetone to syngas. Therefore, if acetone is formed on Ni during steam acetic acid reforming, it would be expected to be converted to syngas rapidly. Coke formed on Ni via ketonisation or condensation, reactions (11)–(15), is therefore unlikely. Thus, the coke deposition under the influence of supported Ni is more likely to involve recombination of unconverted active carbon rich radicals via reaction (16). This coke can be much more graphitised than the coke formed on the support via condensation of ketones. The high oxidation temperature of coke deposits on the catalyst after run 1 (Fig. 8) is thus the result of graphitisation of unconverted active, rich C radicals.

It is remarkable that the overall activity of the catalyst for steam reforming reactions was improved with the recycled catalysts (Fig. 4). Usually the increase in activity (or conversion) is attributed to the increase of number of active sites. From LEIS result, no increase of Ni peak compared with Zr and Ce is observed. Therefore, increase in number of metal particles after recycling is improbable. Importantly, the increase of CO yield is in accordance to the gain of AcOH conversion without any change in yield of CO_2. If the additional acetic acid is converted via decarboxylation route that means $*CH_3$ and CO_2 is made with 1/1 molar ratio. To keep the CO_2 yield constant, all the extra CO_2 has to be consumed. Reactions involving the consumption of CO_2 include dry reforming of hydrocarbon radial and reverse water gas shift (RWGS). Since dry reforming is more difficult than steam reforming, it is not possible that all the additional $*CH_3$ radical is only reformed by CO_2 not by steam. On the other hand, the concentration CO in gas stream is higher than the thermodynamic equilibrium concentration (at 700 °C, 1 atm, selectivity of CO at equilibrium is ~8.3%). Thus, RWGS reaction is not probable. With all those analysis points, additional conversion of acetic acid via decarboxylation as the first step can be ruled out. The route via reaction (9) is not possible either because it also makes CO_2 as the first step. Therefore, the additional acetic acid is probably converted via dehydration route for formation of ketene – reaction (7). Subsequently, ketene can either decompose to CO and methylene by C—–C cleavage via reaction (7) or be converted to acetone by coupling with another ketene to form acetone and CO [30].

There has been a lot of debate about the role of ketene in the mechanism of ketonisation of acetic acid. A recent review by Pham et al. [37] provided a good summary on various proposed mechanisms for this reaction. In typical conditions for ketonisation (e.g., temperatures below 600 °C, only metal oxide as catalyst, long contact times), it usually involves decarboxylation step. Lemonidou et al. [30] investigated TPD of acetic acid on Rh/La_2O_3–$CeZrO_2$ catalyst and found that formation of acetone was followed by CO instead of CO_2. Therefore, they proposed acetone was formed by condensation of two ketene molecules–reaction (19). In the same paper, the decarbonylation of ketene for $*CH_2$ was included as the main pathway of ketene conversion which contributed to reforming activity of the catalyst. We leave the possibility of reaction (19) open here

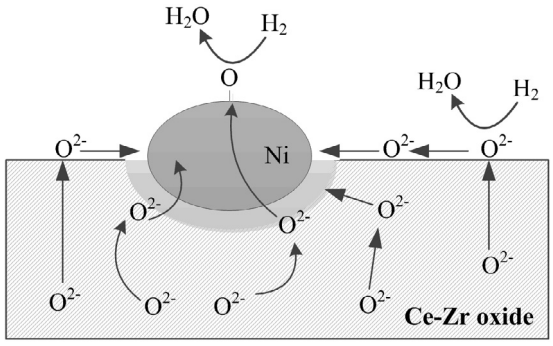

Scheme 2. Migration of oxygen under reductive condition illustrated in the case of H_2. During steam reforming the reducing agents are $*CH_x$ or coke precursor.

since our catalyst system resembles quite well to the one used in that literature. Additionally, the activity improvement can be seen throughout the whole reaction time, above 30 h TOS, this suggests that the gained activity is due to increase of active sites located in the proximity of Ni particles. Thus, the adsorbed intermediates on these sites can be reformed under the influence of Ni. If these intermediates are away from Ni, they tend to form coke which will block these sites after short time on stream. In any scenarios of intermediates on these gained active sites, it is assured that improvement of reducibility of the support can enhance the adsorption of deprotonated acetic acid [35,37]. Also, the CeO_2–ZrO_2 supported Ni catalyst is capable of steam reforming acetone. The recycled catalyst shows ca. 100% conversion of acetone to syngas after 24 h TOS (not shown here).

Another factor which contributes to the higher activity of the recycled catalyst is the capability of minimizing coke deposits on the catalyst. Raman spectroscopy indicates weaker bonds between metal cations and O anion on the recycled catalyst (Fig. 7). This in turn means oxygen becomes more labile and mobile. TPR results are in accordance with Raman result. The support itself becomes easier to be reduced after exposing to steam reforming conditions. Although reduction (in H_2) and oxidation in O_2 can provide certain improvement of redox properties, the presence of oxidative/reductive elements in AcOH steam reforming (e.g., steam, CO_2, coke, acetic acid etc.) seems to make more improvements in the reducibility of the supports. This can be seen even more clearly with the supported Ni catalysts. There is no clear change in TPR profile of fresh catalyst after several oxidation/reduction cycles but surely for the recycled catalysts. In the latter case, the major part of the catalyst support is reduced in the same temperature range of NiO reduction (Fig. 8), implying possible interactions between them. Spill-over of oxygen from the support to Ni particles can probably take place. It should be noted that this phenomena applies for bulk phase migration of O^{2-} anion, *i.e.* oxygen from sub-lattice to the surface and interphase with Ni particles and O from the surface of the mixed oxide to the surface of Ni (illustrated in Scheme 2). As known from literature [38], the migration of O^{2-} from bulk phase to the surface is the rate limiting steps of reduction.

During steam reforming of acetic acid, Ce^{3+} can be re-oxidised by H_2O. The more labile [O] or [OH] on the surface of recycled catalyst can improve the oxidation of the coke precursors absorbed on the support. Moreover, that mobile [O] can spill-over to Ni particles to help the oxidation of carbon radical (e.g. *CH, C* species), thus preventing the graphitisation of coke. The improvement of redox properties results in less coke content, preventing transformation via ageing to hard coke which can be seen from TPO. Lower extend of coking also helps to decrease the deactivation of catalyst.

5. Conclusions

Supported Ni on ceria–zirconia which shows high activity and stability for steam reforming of acetic acid is a potential catalyst for the steam gasification of volatile oxygenates formed from humin during preheating. The steam reforming conditions can modify the metal–oxygen bonds of the oxide support further compared with thermal ageing treatment. Under the reforming conditions, oxygen in the lattice becomes more labile. Thus steam reforming elements (e.g., presence of H_2O, acetic acid, coke, long exposure to reductive/oxidative agents etc.) improve the oxygen mobility of the catalyst, facilitating the redox coupling of Ce^{3+}/Ce^{4+}. The higher activity of recycled catalysts suggests implementation of ageing pre-treatment under reforming conditions can be applied to improve the stability and activity of the catalyst. In addition, the catalyst has high potential for steam reforming of the whole volatile stocks from humin gasification. Since bio-derived oils (e.g., pyrolysis oil, high pressure liquefaction oil) contain similar components to humin volatiles, we strongly believe that this catalyst is also promising for the steam reforming of these bio-oils.

Acknowledgements

This research has been performed within the framework of the CatchBio program Project number 053.70.113. The authors gratefully acknowledge the support of the Smart Mix Program of the Netherlands Ministry of Economic Affairs, Agriculture and Innovation and the Netherlands Ministry of Education, Culture and Science.

References

[1] J.H. Clark, F.E.I. Deswarte, T.J. Farmer, Biofuel. Bioprod. Biorg. 3 (2009) 72–90.
[2] L.H. Zhang, C.B. Xu, P. Champagne, Energ. Convers. Manage. 51 (2010) 969–982.
[3] G.W. Huber, S. Iborra, A. Corma, Chem. Rev. 106 (2006) 4044–4098.
[4] A.J. Ragauskas, C.K. Williams, B.H. Davison, G. Britovsek, J. Cairney, C.A. Eckert, W.J. Frederick Jr., J.P. Hallett, D.J. Leak, C.L. Liotta, J.R. Mielenz, R. Murphy, R. Templer, T. Tschaplinski, Science 311 (2006) 484–489.
[5] T.M.C. Hoang, L. Lefferts, K. Seshan, ChemSusChem 6 (2013) 1651–1658.
[6] T.M.C. Hoang, N. Koteswara Rao, L. Lefferts, K. Seshan, ChemSusChem (2014), submitted.
[7] A.C. Basagiannis, X.E. Verykios, Int. J. Hydrogen Energ. 32 (2007) 3343–3355.
[8] A.C. Basagiannis, X.E. Verykios, Appl. Catal. A: Gen. 308 (2006) 182–193.
[9] A.C. Basagiannis, X.E. Verykios, Appl. Catal. B: Environ. 82 (2008) 77–88.
[10] K. Takanabe, K. Aika, K. Seshan, L. Lefferts, Chem. Eng. J. 120 (2006) 133–137.
[11] B. Matas Güell, I.M. Torres da Silva, K. Seshan, L. Lefferts, Appl. Catal. B: Environ. 88 (2009) 59–65.
[12] B. Matas Güell, I. Babich, K.P. Nichols, J.G.E. Gardeniers, L. Lefferts, K. Seshan, Appl. Catal. B: Environ. 90 (2009) 38–44.
[13] L. An, C. Dong, Y. Yang, J. Zhang, L. He, Renew. Energ. 36 (2011) 930–935.
[14] G. Colón, M. Pijolat, F. Valdivieso, H. Vidal, J. Kašpar, E. Finocchio, M. Daturi, C. Binet, J.C. Lavalley, R.T. Baker, S. Bernal, J. Chem. Soc. Farad. Trans. 94 (1998) 3717–3726.
[15] G. Nahar, V. Dupont, Renew. Sust. Energ. Rev. 32 (2014) 777–796.
[16] F. Fally, V. Perrichon, H. Vidal, J. Kaspar, G. Blanco, J.M. Pintado, S. Bernal, G. Colon, M. Daturi, J.C. Lavalley, Catal. Today 59 (2000) 373–386.
[17] H. Vidal, J. Kašpar, M. Pijolat, G. Colon, S. Bernal, A. Cordón, V. Perrichon, F. Fally, Appl. Catal. B: Environ. 30 (2001) 75–85.
[18] R. Di Monte, J. Kašpar, J. Mater. Chem. 15 (2005) 633.
[19] B. Matas Güell, I.V. Babich, L. Lefferts, K. Seshan, Appl. Catal. B: Environ. 106 (2011) 280–286.
[20] J. Fan, X. Wu, R. Ran, D. Weng, Appl. Surf. Sci. 245 (2005) 162–171.
[21] T. Hirata, J. Phys. Chem. Solids 56 (1995) 951–957.
[22] D.J. Kim, J.W. Jang, H.L. Lee, J. Am. Ceram. Soc. 80 (1997) 1453–1461.
[23] S. Agarwal, L. Lefferts, B.L. Mojet, ChemCatChem 5 (2013) 479–489.
[24] H. Vidal, J. Kašpar, M. Pijolat, G. Colon, S. Bernal, A. Cordón, V. Perrichon, F. Fally, Appl. Catal. B: Environ. 27 (2000) 49–63.
[25] I. Kosacki, T. Suzuki, H.U. Anderson, P. Colomban, Solid State Ionics 149 (2002) 99–105.
[26] R. Si, Y.-W. Zhang, S.-J. Li, B.-X. Lin, C.-H. Yan, J. Phys. Chem. B 108 (2004) 12481–12488.
[27] S. Letichevsky, C.A. Tellez, R.R.d. Avillez, M.I.P.d. Silva, M.A. Fraga, L.G. Appel, Appl. Catal. B: Environ. 58 (2005) 203–210.
[28] M. Kuhn, S.R. Bishop, J.L.M. Rupp, H.L. Tuller, Acta Mater. 61 (2013) 4277–4288.
[29] E.C. Vagia, A.A. Lemonidou, J. Catal. 269 (2010) 388–396.
[30] A.A. Lemonidou, E.C. Vagia, J.A. Lercher, ACS Catal. 3 (2013) 1919–1928.
[31] H. Vidal, S. Bernal, J. Kašpar, M. Pijolat, V. Perrichon, G. Blanco, J.M. Pintado, R.T. Baker, G. Colon, F. Fally, Catal. Today 54 (1999) 93–100.
[32] P. Fornasiero, G. Balducci, R. Di Monte, J. Kašpar, V. Sergo, G. Gubitosa, A. Ferrero, M. Graziani, J. Catal. 164 (1996) 173–183.
[33] K. Takanabe, K.I. Aika, K. Seshan, L. Lefferts, J. Catal. 227 (2004) 101–108.
[34] R. Pestman, R.M. Koster, A. van Duijne, J.A.Z. Pieterse, V. Ponec, J. Catal. 168 (1997) 265–272.
[35] K.S. Kim, M.A. Barteau, J. Catal. 125 (1990) 353–375.
[36] R. Martinez, M.C. Huff, M.A. Barteau, J. Catal. 222 (2004) 404–409.
[37] T.N. Pham, T. Sooknoi, S.P. Crossley, D.E. Resasco, ACS Catal. 3 (2013) 2456–2473.
[38] P. Fornasiero, J. Kašpar, M. Graziani, Appl. Catal. B: Environ. 22 (1999) L11–L14.